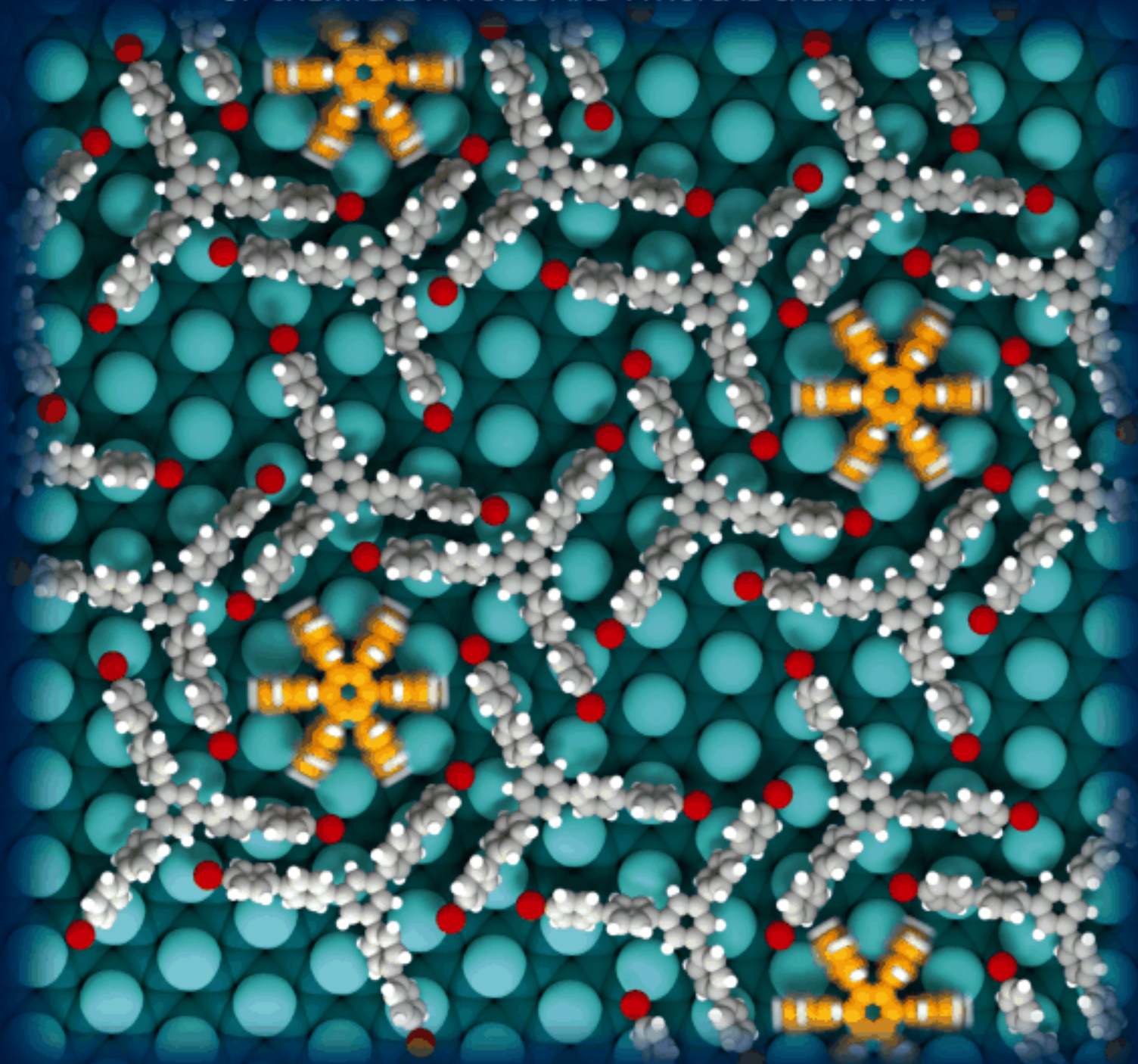


A EUROPEAN JOURNAL

CHEMPHYSCHEM

OF CHEMICAL PHYSICS AND PHYSICAL CHEMISTRY



2/2014

A Journal of



ChemPubSoc
Europe

Artistic representation of thermally activated rotation of pentaphenylbenzene molecules trapped in hexagonal nanopores of a supramolecular network on a SiB(111) surface, suggesting the achievement of molecular machines on semiconducting surfaces, as detailed by F. Palmino et al. on p. 271.

www.chemphyschem.org

WILEY-VCH

DOI: 10.1002/cphc.201301015

Seeding Molecular Rotators on a Passivated Silicon Surface

Oliver Guillermet,^[b, c] Ather Mahmood,^[a] Jianshu Yang,^[b] Jorge Echeverria,^[b] Judicael Jeannoutot,^[a] Sebastien Gauthier,^[b] Christian Joachim,^[b] Frederic Chérioux,^[a] and Frank Palmino*^[a]

Thermally activated rotation of single molecules adsorbed on a silicon-based surface between 77 and 150 K has been successfully achieved. This remarkable phenomenon relies on a nanoporous supramolecular network, which acts as a tem-

plate to seed periodic molecule rotors on the surface. Thermal activation of rotation has been demonstrated by STM experiments and confirmed by theoretical calculations.

1. Introduction

The formation and control of artificial molecular nanomachines adsorbed onto a surface are two of the most promising challenges in nanotechnology.^[1] Among the possible constituents of nanomachines, rotors have attracted particular interest,^[2] and porphyrin-^[3] or phthalocyanine-^[4] based molecules have been widely investigated. These rotors must be coupled to an external energy source in order to get selective-excited rotation in a controlled manner.^[5] Although several studies have shown the usage of chemical,^[6] thermal,^[2b,3] and light^[7] stimuli for producing unidirectional motion or rotation, only a few studies have reported electrically driven rotating units positioned on crystal surfaces.^[3a,8] These rotors are surface-mounted and the excitation and monitoring of such nanomachines is achieved by scanning tunneling microscopy (STM). STM experiments provide not only the tunneling electrons through the tip for excitation but also perform a multitude of tasks including the assembly, monitoring, engineering, and manipulation of molecular machinery bound to the surface. Most of the studies on surface-mounted rotor units by STM have been achieved on noble metal substrates or on a silica surface.^[9] It is possible to develop supramolecular assemblies on semiconductor surfaces without molecule–substrate covalent bonding.^[10] However, to date only a single work that investigates ro-

tator-on-semiconductor surface, that is, with any covalent bond between rotator and surface, has been reported.^[11] This is probably due to the enhanced molecule–substrate interactions between the dangling bonds of the semiconductors and the molecular systems, which could limit the molecular rotation. Nevertheless, from the viewpoint of future hybrid organic/inorganic molecular devices, while molecular interactions with metallic substrates are better understood, semiconducting interfaces are natural choices owing to their wide-range acceptability by the industry.

In the present study we achieve thermally-activated rotation of pentaphenylbenzene (PPB) molecules within nanopores formed in a self-assembled supramolecular network on a silicon-based surface. PPB is composed of five phenyl rings attached to a central aromatic core, where the sixth position on the central ring is vacant. This vacancy works as marker in STM images for an easy identification of static position, step-by-step rotation, and continuous rotation. We demonstrated by STM experiments, performed from 77 to 150 K, and by theoretical calculations that the pore geometry and molecule–surface interactions are key factors in controlling the symmetrical positioning and onset of rotational motion. Furthermore, our ability to control surface temperature allows for the determination of the necessary activation energy to set in motion either individual or groups of these five-lobed rotator structures in the nanoscopic pores.

2. Results and Discussion

To control and observe the rotation at the molecular scale on a semiconductor surface, we need to choose the appropriate molecule/substrate pair. The passivated Si(111)-B surface was used as substrate for the growth of a supramolecular network through template effect. This surface possesses the particularity of showing depopulated silicon dangling bonds due to the presence of boron atoms underneath the top silicon layer.^[10a–h] We chose the PPB molecule as a model of a molecular rotor

[a] Dr. A. Mahmood, J. Jeannoutot, Dr. F. Chérioux, Prof. Dr. F. Palmino
Institut FEMTO-ST, Université de Franche-Comté, CNRS, ENSMM
32 avenue de l'Observatoire, 25044, Besançon cedex (France)
E-mail: frank.palmino@pu-pm.univ-fcomte.fr

[b] Dr. O. Guillermet, Dr. J. Yang, Dr. J. Echeverria, Dr. S. Gauthier,
Dr. C. Joachim
GNS & MANA Satellite
CEMES (Centre d'Elaboration de Matériaux et d'Etudes Structurales)
CNRS, 29 rue Jeanne Marvig, BP 94347, 31055 Toulouse (France)

[c] Dr. O. Guillermet
Université de Toulouse
CEMES (Centre d'Elaboration de Matériaux et d'Etudes Structurales)
CNRS, 29 rue Jeanne Marvig, BP 94347, 31055 Toulouse (France)

 Supporting Information for this article is available on the WWW under <http://dx.doi.org/10.1002/cphc.201301015>.

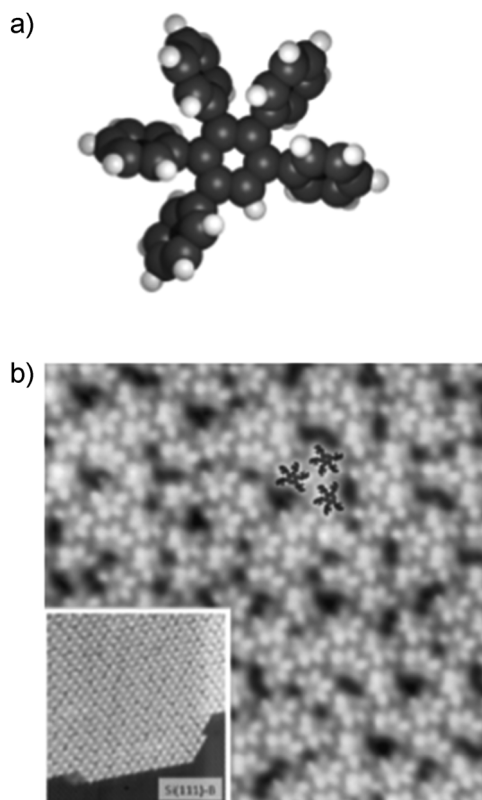


Figure 1. a) Corey Pauling Koltum (CPK) model of pentaphenylbenzene (PPB). b) STM image of PPB deposited on the Si(111)-B surface ($16 \times 16 \text{ nm}^2$, voltage of sample $V_s = -1.6 \text{ V}$, tunnel current $I_t = 10 \text{ pA}$, 100 K), with STM image of an PPB island as an inset ($40 \times 40 \text{ nm}^2$, $V_s = 2.0 \text{ V}$, $I_t = 10 \text{ pA}$, 100 K).

(Figure 1 a). The PPB molecule adopts a propeller shape due to steric hindrance between each lateral phenyl rings, leading to a tilt along the phenyl-phenyl σ -bond axes. This tilt angle lifts the molecule from the surface, reducing the molecule–substrate interaction. This property has been used with similar molecules (hexaphenylbenzene, hexa-*tert*-butylpyrimidopentaphenylbenzene) to achieve the formation of supramolecular self-assemblies^[12] or molecular machines on copper surfaces.^[2a]

The deposition of PPB molecules on a Si(111)-B surface leads to the formation of a compact large-scale non-periodic network (Figure 1 b) and no single molecule is observed on the surface. The molecules are interlocked in the network, maximizing their attractive intermolecular van der Waals interactions. However, this supramolecular arrangement prohibits molecular rotation. In order to circumvent this interlocking, we propose to seclude PPB molecules by using a nanoporous supramolecular network.^[3a] Recently, we have demonstrated that an open network can be obtained by the deposition of 1,3,5-tri(4'-bromo-4,4'-biphenyl)benzene molecules (BPB) on a Si(111)-B surface (see Figure S1 in the Supporting Information).^[10g] Therefore, BPB/Si(111)-B was used as a template to seclude PPB molecules and to investigate PPB molecular rotation inside the nanopores.

PPB molecules were deposited at 300 K onto the BPB/Si(111)-B network and observed by STM at 77 K. The PPB molecules are adsorbed in hexagonal (highlighted by a black circle)

and triangular nanopores (black-dashed circle), as shown in the large-scale STM image of Figure 2a. The PPB five-lobed structure is clearly distinguishable in the triangular nanopores with two of the five lobes appearing slightly darker (Figure 2b). The PPB molecules are randomly adsorbed with three preferential orientations, which could be identified owing to the lacking sixth phenyl ring of the PPB molecules. A bright protrusion appears on the STM image, corresponding to one of the closest arms of the BPB molecules surrounding the PPB molecule (highlighted by a dashed ellipse in Figure 2b). This bright protrusion is rotated by 120° in the three different cases indicating its relation to the molecule orientation inside the triangle nanopore (Figure 2b).

In the case of hexagonal nanopores (Figure 2c), the PPB molecules five-lobed structure is still recognizable, one lobe being darker than the other four, and it appears to be centered in the hexagonal pores. There are six possible PPB molecule orientations, which are all observed in the large-scale STM images (see Figure S2).

From our previous work concerning the formation of large-scale supramolecular network by BPB molecules deposition on a Si(111)-B surface,^[10f–g] and from the high-resolution STM images (Figure 2) the adsorption sites of the PPB molecules in the triangles and hexagons can be determined.

In each triangle nanopore there are three silicon adatoms and consequently, three possible orientations rotated by 120° relative to each other. Two of the five lateral phenyl rings are located above the other two silicon adatoms of the triangle (Figure 3).

The other three lateral phenyl rings point towards two surrounding BPB molecules. One of these phenyl groups is closer to the arms of the neighboring molecule than the other. This effect could be the origin of the brightest protrusions observed in the STM image (see dashed ellipse in Figure 2b). A bromophenyl group of a third BPB molecule is interdigitated with the PPB molecule due to the vacancy on the sixth position on the central ring. The stability of the PPB/BPB/Si(111)-B interface below 107 K is explained by both molecule–molecule and molecule–substrate interactions.

For PPB molecules adsorbed in hexagons, the adsorption site is also defined by the analysis of high resolution STM images. By tracing lines joining two protrusions attributed to opposite bromophenyl groups of the BPB molecule (see Figure S3), it can be seen that 1) the center of the PPB molecule is placed exactly at the center of the hexagon, with its central phenyl ring on top of the central Si atom and that 2) the PPB molecules are rotated by 12° with respect to the network BPB/Si(111)-B. Due to the sixfold symmetry of hexagonal nanopores, there is a single adsorption site for the PPB molecules in these nanopores, but with six possible orientations that can be obtained by rotations of 60° relative to each other. In this adsorption model, each lateral phenyl group of the PPB molecule is located between two silicon adatoms (Figure 3).

In the subsequent part of this manuscript, the temperature effect is only investigated for PPB adsorbed in hexagonal nanopores. At 130 K, the PPB molecule can be adsorbed in a hexagonal pore in one of the six possible orientations (Figure 4a).

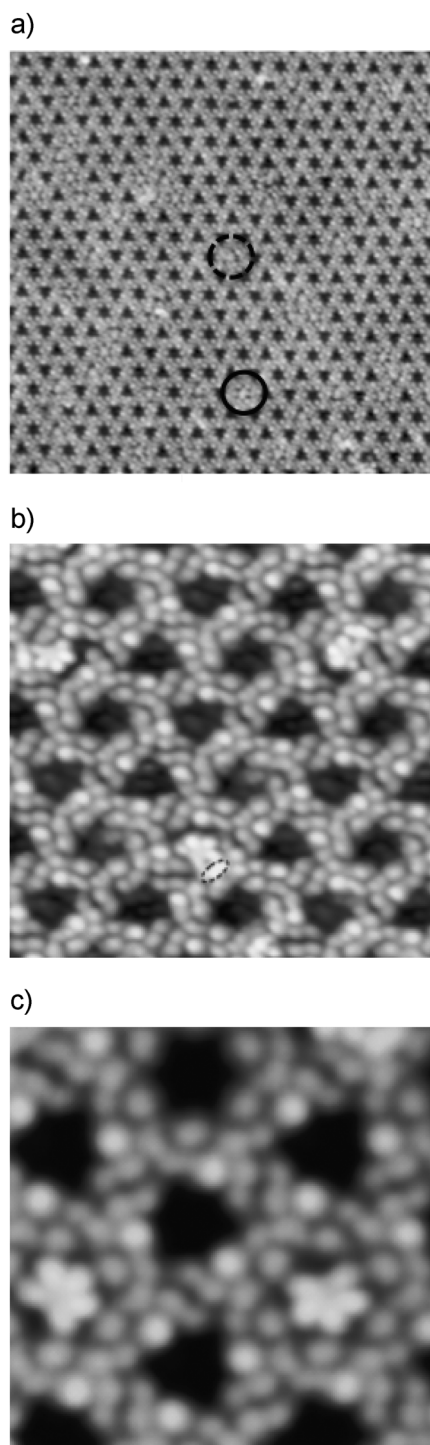


Figure 2. a) Large-scale STM image of PPB on a BPB supramolecular network on a Si(111)-B surface ($60 \times 60 \text{ nm}^2$, $V_s = -2.1 \text{ V}$, $I_t = 10 \text{ pA}$, 77 K). Examples of PPB molecules adsorbed in a triangle and in a hexagon are highlighted by a dashed black circle and by a dark circle, respectively. b) STM image of three PPB molecules adsorbed in three triangular nanopores of BPB/Si(111)-B, rotated by 120° one from each other ($5.5 \times 5.5 \text{ nm}^2$, $V_s = -2.0 \text{ V}$, $I_t = 10 \text{ pA}$, 107 K). The dashed ellipse highlights a bright protrusion corresponding to the BPB molecule closest to a PPB molecule. c) STM image showing two PPB molecules adsorbed in hexagonal nanopores of BPB/Si(111)-B representing two of the six possible orientations in the hexagons ($6 \times 6 \text{ nm}^2$, $V_s = -2.1 \text{ V}$, $I_t = 3 \text{ pA}$, 77 K).

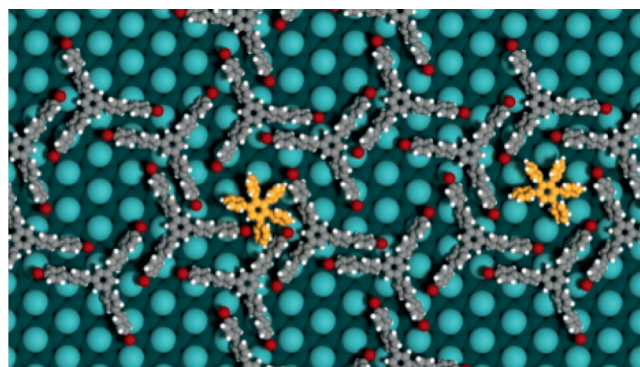


Figure 3. Adsorption model of a PPB molecule in a triangle nanopore (left) and in a hexagon nanopore (right) of the BPB/Si(111)-B network. Si atoms are shown as light blue balls and Si bulk atoms as dark blue balls.

After 130 s, the PPB molecule looks the same but it is clockwise rotated by 60° (Figure 4b). With a delay of further 130 s, this very PPB molecule is again rotated by 60° in clockwise direction (Figure 4c). The rotation direction is only apparent because a study of a large number of STM images shows that the molecules rotate both in clockwise and counterclockwise direction without any preference.

At 150 K, the image of the PPB molecules that are trapped in the hexagonal pores changes markedly, as displayed in Figure 5.

They now appear blurred, because they often move in a time interval of 0.512 s separating two horizontal scan lines. Note that the BPB network and the molecules trapped in the triangular pores do not move during this time. The abrupt jumps that appear between consecutive scan lines are strictly located in the hexagonal cavities. Note that the molecule that is visible in the top right of Figure 5 appears to have six lobes. This effect, which has already been observed in a fivefold symmetric molecule^[13] stems from the fact that the image combines several partial images of the immobile molecule. These six-lobe molecules were repeatedly observed at 150 K (see Figure S4).

This analysis suggests that the PPB molecules rotate around an axis defined by the central Si atom of the hexagonal pores. This rotation is completely frozen below 77 K (Figure 2), while single rotation events are imaged on the time scale of a full image at 130 K (Figure 4). At 150 K, the rotation events are more frequent; they happen on a time scale given by the fast scanning direction period (Figure 5). A thermally activated rotational process is expected to follow the Arrhenius law shown in Equation (1):

$$\Gamma_{\text{rot}} = A \exp(-E_{\text{rot}}/kT) \quad (1)$$

where Γ_{rot} is the rotation rate, A the prefactor, and E_{rot} the rotational energy barrier.^[2b] A rough estimation of the energy barrier can be deduced from our measurements. Considering that the mean time of residence of a PPB molecule in one orientation is of the order of 100 s at 130 K (Figure 4) and 1 s at 150 K (Figure 5), Equation (1) leads to an activation barrier $E_{\text{rot}} =$

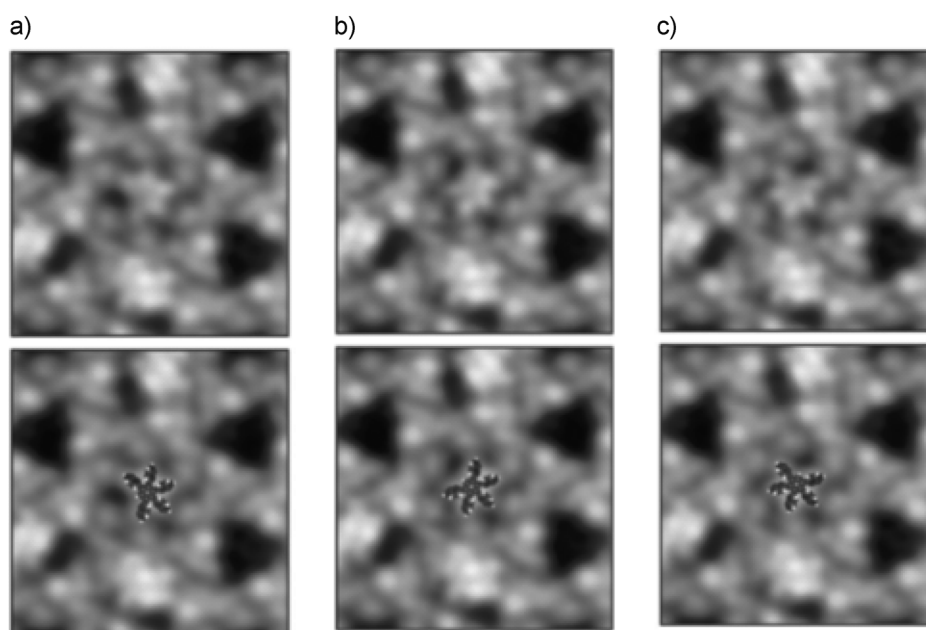


Figure 4. STM images of the same area of a PPB/BPB/Si(111)-B network at 130 K ($2.8 \times 2.8 \text{ nm}^2$, $V_s = -2 \text{ V}$, $I_t = 10 \text{ pA}$). a) The PPB molecule is adsorbed in a hexagon nanopore and appears as a five-lobe structure. b) After 130 s, the same PPB molecule appears still as a five-lobe structure but rotated clockwise by 60° . c) STM image recorded after 5 min. The PPB molecule is again rotated clockwise by 60° with respect to the previous STM image shown in (b).

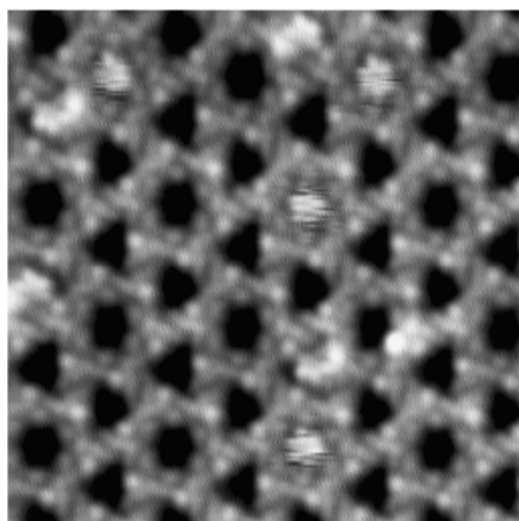


Figure 5. STM image of the PPB/BPB/Si(111)-B interface at 150 K showing PPB molecules adsorbed in hexagonal pores at 150 K ($11 \times 11 \text{ nm}^2$, $V_s = -2,1 \text{ V}$, $I_t = 5 \text{ pA}$). The fast scanning period (horizontal direction) is 0.512 s.

0.37 eV with a prefactor $A = 10^{13} \text{ s}^{-1}$. These values are very close to those of Barth et al. in the case of organic molecules trapped in a supramolecular network on a Ag(111) surface.^[2b]

In recent years, theoretical calculations have proved to be a very useful tool for the study of rotary molecular motors.^[14] To confirm the barrier height, molecular mechanics and dynamics calculations were performed using the ASED+ semi-empirical technique^[15] considering orbital and van der Waals

interactions between the adsorbed molecules and the surface. First, the Si(111)-B surface was optimized with six BPB molecules forming a hexagonal nanopore. Then, a PPB molecule was placed at the center of this nanopore and its geometry optimized. In the resulting conformation, the central Si adatom can act as a rotation axis for the PPB molecule by holding its central benzene ring (See Figure S5). By forcing the PPB molecule to rotate in steps of one degree, the minimal energy path of the rotation process was determined. One could also calculate the complex potential energy surface of this rotation process; however, there are too many degrees of freedom for this molecular system, which render the representation of the complete rotational potential energy surface as a function of all conformation angles involved infeasible.

At a very low surface temperatures (i.e. 1 K) and on the simplified potential energy surface, calculating a minimal energy path for a given rotation trajectory leads to six large maxima per PPB turn on the rotational potential energy profile (Figure 6).

This sequence of six maxima corresponds to the 60° switching observed in the experiments due to the sixfold symmetry of the substrate surface. The calculated energy barrier has a height between 0.4 and 0.6 eV, in fair agreement with the rough experimental evaluation discussed previously. This barrier height is mainly due to the molecule–surface interaction, as the five phenyl arms of the PPB molecule interact strongly with the six Si adatoms present in the hexagonal pore, but they do it to a lesser extent with the surrounding BPB molecules. On the contrary, the small peaks observed on the rotational potential energy curve (Figure 6) are due to the lateral re-orientations of the five phenyl rings of PPB when they are located in between two Si adatoms (see video in the Supporting Information).

The calculated rotational energy curve has the characteristics of a ratchet-like mechanical machinery with strong asymmetry. This asymmetry is not intrinsic, it was introduced by imposing a pre-determined rotation trajectory of the PPB molecule while searching for the minimal energy path. In the ASED+ calculations, increasing the surface temperature has the effect of starting a random PPB rotation when kT is large enough to overcome the calculated energy barrier. Of course, it is however not possible to control the PPB direction of rotation with only such thermal noise, not even with the asymmetric potential shown in Figure 6.^[16]

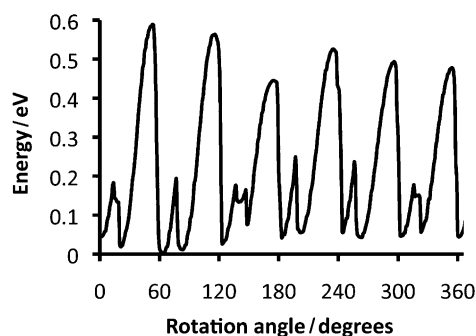


Figure 6. Rotational potential energy curve of a PPB located in a hexagonal pore of a Si(111)-B surface decorated with a BPB supramolecular network. This energy profile results from a step-by-step energy minimization of the complete molecular system at 1 K while imposing a rotation of the PPB molecule around the central atop Si atom.

3. Conclusions

We have observed thermal activation of rotation of single molecule-rotators at 130 K on a silicon-based surface by using a passivated semiconductor and a nanoporous supramolecular network acting as a template to stabilize and isolate one molecule-rotor from the other on the surface. The rotational energy barrier of molecular rotators is mainly due to the molecule–surface interaction. We think that this study opens new avenues for studying the controlled dynamics of molecular machines fabricated on semiconducting surfaces.

Experimental Section

Additional STM images, experimental procedures and calculations are fully described in the Supporting Information.

Acknowledgements

This work was supported by the Pays de Montbéliard Agglomération and the French agency Agence Nationale de la Recherche (ANR-09-NANO-40). The authors thank Sébastien Coget (Institut FEMTO-ST) for the realization of animated graphics with Blender software and Dr. Sarah Benchabane (Institut FEMTO-ST) for fruitful discussion.

Keywords: molecular rotator • scanning probe microscopy • silicon surface • simulation • supramolecular chemistry

- [1] a) D. Lensen, J. A. A. W. Elemans, *Soft Matter* **2012**, *8*, 9053–9063; b) U. G. E. Perera, F. Ample, H. Kersell, Y. Zhang, G. Vives, J. Echeverria, M. Grisolia, G. Rapenne, C. Joachim, S.-W. Hla, *Nat. Nanotechnol.* **2013**, *8*, 46–51; c) G. S. Kottas, L. I. Clarke, D. Horinek, J. Michl, *Chem. Rev.* **2005**, *105*, 1281–1376; d) B. L. Feringa, *Acc. Chem. Res.* **2001**, *34*, 504–

- 513; e) J. A. Stroschio, D. M. Eigler, *Science* **1991**, *254*, 1319–1326; f) T. A. Jung, R. R. Schlittler, J. K. Gimzewski, H. Tang, C. Joachim, *Science* **1996**, *271*, 181–184.
- [2] a) F. Chiaravalloti, L. Gross, K.-H. Rieder, S. M. Stojkovic, A. Gourdon, C. Joachim, F. Moresco, *Nat. Mater.* **2007**, *6*, 30–33; b) D. Kühne, F. Klappenberger, W. Krenner, S. Klyatskaya, M. Ruben, J. V. Barth, *Proc. Natl. Acad. Sci. USA* **2010**, *107*, 21332–21336; c) J. K. Gimzewski, C. Joachim, R. R. Schlittler, V. Langlais, H. Tang, I. Johanssen, *Science* **1998**, *281*, 531–533; d) B. C. Stipe, M. A. Rezaei, W. Ho, *Science* **1998**, *279*, 1907–1909.
- [3] a) N. Wintjes, D. Bonifazi, F. Cheng, A. Kiebele, M. Stöhr, T. A. Jung, H. Spillmann, F. Diederich, *Angew. Chem.* **2007**, *119*, 4167–4170; *Angew. Chem. Int. Ed.* **2007**, *46*, 4089–4092; b) M. Wahl, M. Stöhr, H. Spillmann, T. A. Jung, L. H. Gade, *Chem. Commun.* **2007**, 1349–1351; c) D. Écija, W. Auwärter, S. Vijayaraghavan, K. Seufert, F. Bischoff, K. Tashiro, J. V. Barth, *Angew. Chem.* **2011**, *123*, 3958–3963; *Angew. Chem. Int. Ed.* **2011**, *50*, 3872–3877.
- [4] a) T. Ye, T. Takami, R. Wang, J. Jiang, P. S. Weiss, *J. Am. Chem. Soc.* **2006**, *128*, 10984–10985; b) J. Otsuki, Y. Komatsu, D. Kobayashi, M. Asakawa, K. Miyake, *J. Am. Chem. Soc.* **2010**, *132*, 6870–6871.
- [5] W. R. Browne, B. L. Feringa, *Nat. Nanotechnol.* **2006**, *1*, 25–35.
- [6] T. R. Kelly, H. D. Silva, R. A. Silva, *Nature* **1999**, *401*, 150–152.
- [7] N. Koumura, R. W. J. Zijlstra, R. A. van Delden, N. Harada, B. L. Feringa, *Nature* **1999**, *401*, 152–155.
- [8] a) H. L. Tierney, C. J. Murphy, A. D. Jewell, A. E. Baber, E. V. Iski, H. Y. Khodavernian, A. F. McGuire, N. Klebanov, E. C. H. Sykes, *Nat. Nanotechnol.* **2011**, *6*, 625–629; b) B. V. Rao, K.-Y. Kwon, A. Liu, L. Bartels, *Proc. Natl. Acad. Sci. USA* **2004**, *101*, 17920–17923.
- [9] a) L. I. Clarke, D. Horinek, G. S. Kottas, N. Varaksa, T. F. Magnera, T. P. Hinderer, R. D. Horansky, J. Michl, J. C. Price, *Nanotechnology* **2002**, *13*, 533–540; b) G. London, G. T. Carroll, B. L. Feringa, *Org. Biomol. Chem.* **2013**, *11*, 3477–3483.
- [10] a) Y. Makoudi, M. Arab, F. Palmino, E. Duverger, C. Ramseyer, F. Picaud, F. Chérioux, *Angew. Chem.* **2007**, *119*, 9447–9450; *Angew. Chem. Int. Ed.* **2007**, *46*, 9287–9290; b) Y. Makoudi, F. Palmino, E. Duverger, M. Arab, F. Chérioux, C. Ramseyer, B. Therrien, M. J.-L. Tschan, G. Süß-Fink, *Phys. Rev. Lett.* **2008**, *100*, 076405; c) Y. Makoudi, F. Palmino, M. Arab, E. Duverger, F. Chérioux, *J. Am. Chem. Soc.* **2008**, *130*, 6670–6671; d) M. El Garah, Y. Makoudi, E. Duverger, F. Palmino, A. Rochefort, F. Chérioux, *ACS Nano* **2011**, *5*, 424–428; e) B. Baris, V. Luzet, E. Duverger, P. Sonnet, F. Palmino, F. Chérioux, *Angew. Chem.* **2011**, *123*, 4180–4184; *Angew. Chem. Int. Ed.* **2011**, *50*, 4094–4098; f) Y. Makoudi, B. Baris, J. Jeannoutot, F. Palmino, B. Grandidier, F. Chérioux, *ChemPhysChem* **2013**, *14*, 900–904; g) B. Baris, J. Jeannoutot, V. Luzet, F. Palmino, A. Rochefort, F. Chérioux, *ACS Nano* **2012**, *6*, 6905–6911; h) S. R. Wagner, R. R. Lunt, P. Zhang, *Phys. Rev. Lett.* **2013**, *110*, 086107; i) K. R. Harikumar, T. Lim, I. R. McNab, J. C. Polanyi, L. Zotti, S. Ayissi, W. A. Hofer, *Nat. Nanotechnol.* **2008**, *3*, 222–228; j) P. A. Sloan, R. E. Palmer, *Nature* **2005**, *434*, 367–371.
- [11] Y. W. Mo, *Science* **1993**, *261*, 886–888.
- [12] L. Gross, F. Moresco, P. Ruffieux, A. Gourdon, C. Joachim, K.-H. Rieder, *Phys. Rev. B* **2005**, *71*, 165428.
- [13] E. Niemi, S. Nagarajan, X. Bouju, D. Martrou, A. Gourdon, S. Gauthier, O. Guillermet, *Angew. Chem.* **2009**, *121*, 2004; *Angew. Chem. Int. Ed.* **2009**, *48*, 1970.
- [14] C. García-Iriepa, M. Marazzi, F. Zapata, A. Valentini, D. Sampedro, L. M. Frutos, *J. Phys. Chem. Lett.* **2013**, *4*, 1389.
- [15] F. Ample, C. Joachim, *Surf. Sci.* **2006**, *600*, 3243–3251.
- [16] R. D. Astumian, *Science* **1997**, *276*, 917–922.

Received: November 4, 2013